A Journal of the Gesellschaft Deutscher Chemiker

Angewandte International Edition GDCh Chemie

www.angewandte.org

Accepted Article

Title: A novel class of 1H-MRI Contrast Agents based on the relaxation enhancement induced on water protons by 14N imidazole moieties

Authors: Simonetta Geninatti Crich, Simona Baroni, Rachele Stefania, Lionel M. Broche, Nicholas Senn, David J. Lurie, James J. Ross, and Silvio Aime

To be cited as: *Angew. Chem. Int. Ed.* 10.1002/anie.202011513

Link to VoR: https://doi.org/10.1002/anie.202011513

WILEY-VCH

10.1002/anie.202011513

WILEY-VCH

RESEARCH ARTICLE

A novel class of ^{1}H-MRI Contrast Agents based on the relaxation enhancement induced on water protons by ^{14}N imidazole moieties

S. Baroni,† R. Stefania,† L. M. Broche, N. Senn, D. J. Lurie, P. J. Ross, S. Aime, S. Geninatti Crich*

[a] Dr. S. Baroni†, Dr. R. Stefania, Prof. S. Aime, Prof. S. Geninatti Crich*
Department of Molecular Biotechnology and Health Sciences, University of Torino, via Nizza 52, Torino, Italy
via Nizza 52, 10126, Torino (Italy)
E-mail: simonetta.geninatti@unito.it
[b] Dr. L.M. Broche, Dr. N. Senn, Prof. D.J. Lurie, Dr. J. Ross
Aberdeen Biomedical Imaging Centre,
University of Aberdeen,
Foresterhill, AB25 2ZD, Aberdeen, U.K
[c] Prof. S. Aime
Istituto di Biostrutture e Bioimmagini (IBB), CNR,
via Nizza 52, 10126, Torino (Italy)

† These authors contributed equally to this work.

Supporting information for this article is given via a link at the end of the document.

Abstract: This study aims at developing a completely new class of MRI contrast agents, displaying remarkable relaxation effects in the absence of paramagnetic metal ions. Their detection requires the acquisition of images at variable magnetic field strength as provided by Fast Field Cycling imaging scanners. They contain poly-histidine chains (poly-His), whose imidazole groups generate ^{14}N-Quadrupolar-Peaks that cause a relaxation enhancement of water protons at a frequency (1.38±0.3 MHz) that is readily detectable from the frequencies associated with endogenous proteins. The poly-His QPs are detectable only when the polymer is in a solid-like form, i.e. at pH > 6.6. Above this value, their intensity is pH dependent and can be used to report on the occurring pH changes. On this basis, the poly-His moieties were conjugated to biocompatible polymers such as polylactic and glycolic acid, in order to form stable nanoparticles able to encapsulate structured water in their core. FFC images were acquired to assess their contrast-generating ability.

Introduction

In the last few decades, Magnetic Resonance Imaging (MRI) has become one of the key modalities in clinical settings thanks to its superb spatial resolution and its outstanding ability to differentiate soft tissues. The contrast in an MR image arises mainly from differences in the relaxation times (T_1 and T_2) of tissue water protons, as a consequence of their interaction with macromolecules, paramagnetic metal ions and biological membranes. On this basis, it was rather straightforward in the 1980s to seek MRI contrast agents in the field of paramagnetic systems, whose ability to shorten the water proton relaxation rates was already well established [1]. The Gd(III) ion with its seven unpaired electrons and its (relatively) long electronic relaxation time was quickly identified as the candidate of choice for this application. As free Gd(III) ions are toxic for biological systems, it was suggested to use Gd-containing complexes with octadentate ligands that wrap around the metal ion leaving one coordination site available for the coordination of a water molecule in fast exchange with "bulk" water [2,3]. Thus Gd-Based Contrast Agents (GBCAs) yield an increase of water proton relaxation rates in the regions where they distribute. Currently, about 40% of the MRI scans carried out in clinical settings make use of GBCAs [4]. They are quickly excreted from the patients' bodies after i.v. administration at doses of 0.1-0.3 mmol/kg with a $t_{1/2}$ of the order of one hour. In recent years, it has been shown that tiny amounts of Gd may be retained in the tissues of patients injected with GBCAs [5]. Although clinical consequences have been reported only in the case of patients with impaired renal function, these observations bring a growing concern about the use of GBCAs [6–8]. Thus, probe developers are urgently challenged to find alternatives to GBCAs [9–11]; the problems raised by GBCAs suggest addressing routes that do not involve metal complexes. Meanwhile, researchers' attention is also devoted to the search for innovative solutions that could allow *in vivo* applications that would not have been possible using GBCAs.

In the search for alternatives to GBCAs (and related paramagnetic complexes based on Mn(II), Mn(III) or Fe(III)) we were inspired by the relaxation enhancement brought about by "semi-solid" proteins in biological tissues [12,13]. In fact, "relaxation enhancement peaks" at specific values of applied magnetic field were reported early in the NMR study of immobilized proteins [14,15], as well in the case of biological tissues. The occurrence of these peaks is readily detectable at defined frequencies in the Nuclear Magnetic Relaxation Dispersion (NMRD) curve of the investigated specimen [16–18], and were associated with the amide functionalities of immobilized (semi-solid) proteins as the relaxation enhancement occurs at the magnetic fields where the proton NMR frequency coincides with the frequency of the ^{14}N nuclear quadrupole resonance (NQR) of the amide groups. These relaxation enhancement peaks were therefore deemed "^{14}N quadrupolar peaks" (^{14}N-QPs, Figure 1). We surmised that other ^{14}N containing functionalities may be the source for proton relaxation enhancements at frequencies different from those reported for the protein amide groups. This approach may lead to a novel class of "frequency-encoding" agents that eventually may prompt the development of MRI scanners operating at magnetic fields very different to the ones (typically 1.5 T or 3.0 T) currently

10.1002/anie.202011513

employed for *in vivo* studies. Ideally, the frequency-encoding agents would be the best candidates for Fast Field-Cycling (FFC) imaging scanners [19,20] as the subtraction of images acquired at different magnetic fields may allow one to fully exploit the potential associated with the field-dependence of proton relaxation rates. An additional difference with GBCAs arises from the need to work with immobilized systems, as ^{14}N-QPs disappear completely when the agent is in the solution state [18]. Therefore, one has to envisage moieties that act as contrast agents when they are under the form of particles or even as components of implant devices such as scaffolds for regenerative medicine applications. Herein we report our observations on imidazole-containing peptides that appear to be excellent representatives of this novel class of MRI ^{14}N-QP-based contrast agents.

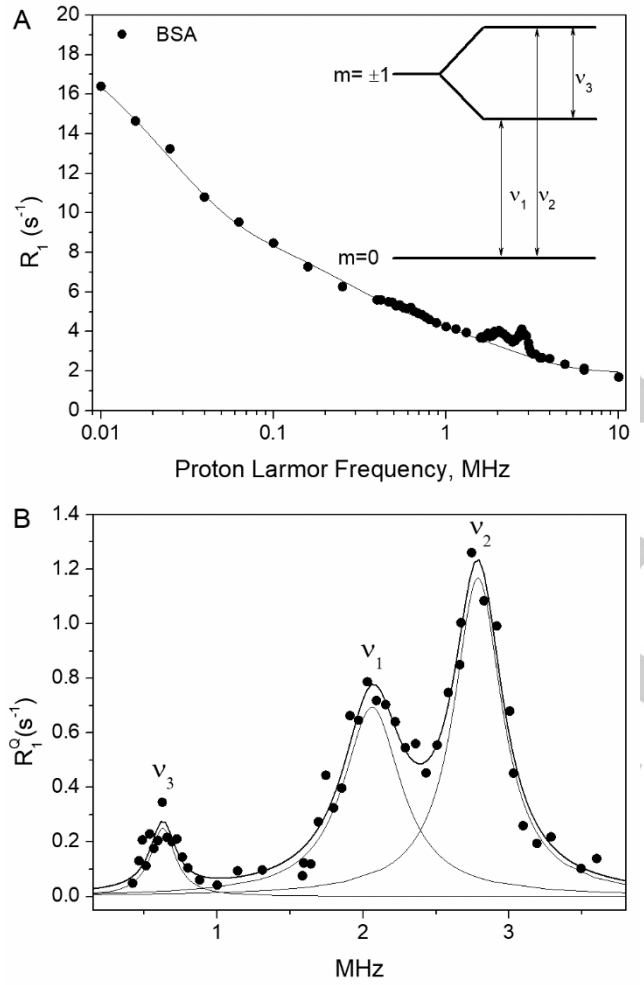

Figure 1. NMRD profile of immobilized protein. (**A**) NMRD profile of cross-linked Bovine Serum Albumin (BSA) with a multi-exponential decay to background dispersion, excluding data in the QP ranges. In the inset, the energy levels of ^{14}N nuclei (S ≥ 1) due to QP interactions with local electric field gradients are reported. The two levels to the left occur for axial symmetry. The upper level splits when the axial symmetry is broken, as shown to the right. A local maximum of the R_1 profile of protons occurs when the Zeeman transition energy of the proton spin is equal to the energy difference of two levels of the S spin. (**B**) Lorenzian fits to the QPs.

In the case of biological tissues, the ^{14}N-QPs are detected at the proton NMR frequencies of 0.7, 2.1 and 2.8 MHz, equivalent to field strengths of 16 mT, 49 mT and 65 mT [18]. For such systems, it is well established that the detection of the QPs is associated with the presence of endogenous amidic peptide groups. Furthermore, it was shown that the amplitude of the ^{14}N-QPs is proportional to the amount of protein present in the considered specimen [21]. This observation prompted investigations aimed at showing that the detection of ^{14}N-QPs may act as a reporter of an ongoing pathology that affects the amount and mobility of the associated proteins. The present work shows how it is possible to develop an innovative class of MRI contrast agents based on the generation of detectable ^{14}N-QPs that fall at frequencies well-distinct from those generated from the amidic peptide functionalities of the endogenous proteins. Thus, the QPs arising from the exogenous contrast agent can be easily identified and their detection will not be affected by the presence of endogenous QPs.

Results

The proof-of-concept of generating ^{14}N-QPs different from those due to the tissues' immobilised proteins was achieved by using an aqueous suspension of particles of poly-histidine polymer. Unlike all the immobilized proteins or specimens of biological tissues reported to date in the literature, the NMRD of poly-Histidine (poly-His, Figure 2A) showed a characteristic relaxation peak at 1.38 MHz due to the ^{14}N nuclear quadrupole resonance frequency of the imidazole groups present on the polymeric chain [22]. Two additional ^{14}N-QPs from the imidazole group appear as broad peaks at about 0.98 and 0.7 MHz, respectively, but they are not useful for the intended application because of the overlap with the ^{14}N-QPs at 0.7 MHz arising from the tissue protein amidic groups. Figure 2B reports the NMRD profile of poly-His (MW= 15,600, dispersed in water at 30%$_{w/w}$), showing the characteristic ^{14}N-QPs that are compared with the NMRD profile of an *ex vivo* fresh muscle tissue from a BALB/c mouse.

The ^{14}N-QP at 1.38±0.5 MHz arising from the imidazole groups is readily detectable and distinct from the QPs generated by the background tissue (figure 2C and 2D).

The increase of water proton relaxation rate (ΔR_1) and the relaxation enhancement were calculated using the following equations:

$$\Delta R_1 = R_1^{1.38MHz} - R_1^{1.65MHz} \ (s^{-1}) \qquad \text{Equation 1}$$

$$relaxation\ enhancement = \Delta R_1 / R_1^{1.65MHz} * 100 \qquad \text{Equation 2}$$

Where the relaxation rate at 1.38 MHz and 1.65 MHz correspond to the top and the base values of the imidazole peak of poly-His, respectively.

The relaxivity enhancement of poly-His was *ca*. 70% corresponding to a $\Delta R_1 \sim 6\ s^{-1}$.

NMRD profiles acquired on specimens at different poly-His concentrations are reported as Supplementary Materials (Figure S1). Although the ^{14}N-QP at 1.38 MHz still remained detectable at the lowest tested concentration (5 mg/ml), we suggest that the 14 mg/ml concentration, corresponding to a relaxation enhancement of 49% and a ΔR_1 of 0.4 s^{-1}, should represent a reasonable threshold in the presence of a consistent tissue background.

10.1002/anie.202011513

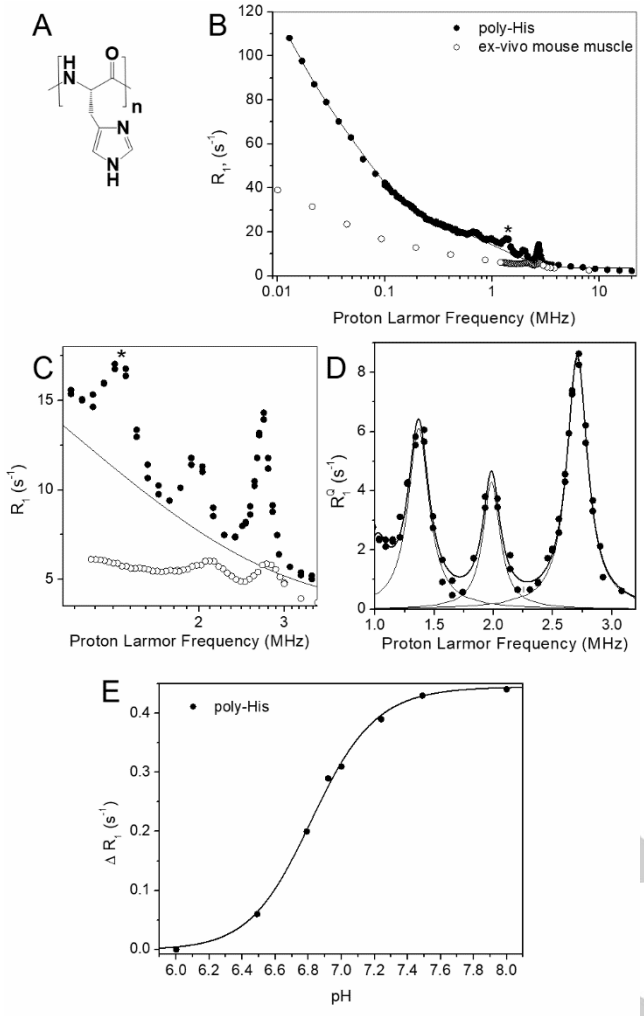

Figure 2. The poly-His. (A) Schematic representation of poly-His. (B) NMRD profile acquired from 0.01 to 20 MHz of poly-His (30% w/w) in water (●) compared with the NMRD profile of an ex vivo fresh muscle tissue (○) from BALB/c mouse (T=25°C). A multi exponential decay fitting to background dispersion, excluding data in the QP ranges, was performed for poly-His (black line). The asterisk * identifies the imidazole peak in the side-chain of poly-His. Expansion of the QPs region before (C) and after (D) the background subtraction with Lorenzian fits to the QPs. (E) The ΔR1 of the 14N-QP peak (equation 1) as a function of the pH, for a 15 mg/ml poly-His sample. The line is to guide the eyes.

Assessment of pH dependence of ^{14}N-QPs.

As pH controls the physical state of the poly-His solid/liquid status and given that the ^{14}N-QPs are only observed for immobilized systems [16], changes in the intensity of the imidazole QPs can act as a reporter of the pH of the microenvironment. In fact, the protonation of the imidazole group of the histidine (pK_a=6.8)[23,24] increases the polymer solubility with a consequent increase in mobility and progressive disappearance of the QPs (Figure 2E).

Poly-Histidine containing nanoparticles.

As the appearance of the ^{14}N-QPs is associated with an immobilized physical state of the moiety generating the proton relaxation enhancement of the surrounding water molecules, nano- or micro-particles represent a suitable form for the new class of contrast agent. We have pursued the task of generating nanoparticle-based contrast agents by confining the poly-His chains responsible for the ^{14}N-QPs inside a biocompatible nanoparticle. In fact, the overall dynamics of the imidazole-containing chain has an important role in the generation of the ^{14}N-QPs and the immobilization of the polymeric chains in a tissue-like state is mandatory. Accordingly, an oligopeptide containing 15 histidines was conjugated to polylactic and glycolic acid (PLGA) co-polymers to yield hybrid nanoparticles (Figure 3 and Supplementary Materials, Figure S2-S6). PLGA is approved by the US Food and Drug Administration (FDA) and the European Medicine Agency (EMA) in several drug delivery systems for human use [25,26]. These polymers are commercially available at different molecular weights and copolymer compositions. Furthermore, the interior of PLGA nanoparticles (PLGA-NPs) is accessible to bulk water to an extent that is inversely proportional to the size of the NP [27,28]. In order to allow the incorporation of many histidine units into the PLGA-NP, an oligo-His peptide (amino acid sequence: $CGGH_n\beta A$, n=15) was synthesized by Solid Phase Peptide Synthesis (SPPS) using the Fmoc strategy. The NMRD profile of the oligo-His peptide suspension was not significantly different from that obtained from the commercial polyaminoacid sample (ca. 114 residues, see Supplementary Materials, figure S7).

Then, the oligo-His peptide was conjugated to the PLGA-PEG_2-maleimide derivative, through the coupling between the N-terminal cysteine residue (C) and the maleimide terminal groups of PEG, following the procedure as described in figure 3. The chemical structure of the final product oligo-His-PLGA was confirmed by ^{1}H-NMR spectra (see Supplementary Materials, figure S6). The PLGA-NPs were obtained by applying the oil/water (o/w) emulsion solvent extraction method.[27] The organic phase was prepared by dissolving the oligo-His-PLGA and the PLGA Resomer® RG 502 H (1:1) in chloroform:methanol (75:25). The water phase was a PolyVinyl Alcohol (PVA) aqueous solution (3%). PVA is the most commonly-used emulsifier for the preparation of PLGA-NPs because it yields particles that are relatively uniform, small sized, and which can be easily re-dispersed in water.[29] The average hydrodynamic diameters of the oligo-His-PLGA-NPs were determined by dynamic light scattering (DLS) measurements, and were equal to ca. 150 nm (157 ± 2 nm). The NMRD profile acquired on suspensions containing oligo-His-PLGA-NPs (at a 5 mg/ml oligo-His concentration) is reported in Figure 4. It showed that the imidazole QP is more pronounced (ΔR_1=0.20 s^{-1}, +67%) than the corresponding one obtained for the commercial poly-His at the same concentration (ΔR_1 = 0.12 s^{-1}). Profiles acquired in the pH range 5.5-7.4 showed the same pH dependence of Oligo-His-PLGA QPs intensity observed with poly-His (Figure 2E), with a slight shift toward more acid pHs (Figure S8).

***In vivo* ^{14}N-QPs detection of oligo-His-PLGA-NPs in murine tumour xenograft.**

In order to test whether the QP generated by poly-histidine based contrast agents could be detected *in vivo* in tumour animal models, the NMRD profiles were acquired using a prototype FFC relaxometer endowed with a wide-bore magnet, sufficient to accommodate mice of 20-25 g [30]. Due to the absence of spatial resolution, in order to excite a small, well-defined volume containing the tumour region, a surface microcoil of elliptical shape defined by 3 and 2 mm axes (Area = 4.71 mm^2) was used. The penetration depth of the coil is about 1.5 mm (Figure 5A). For this purpose 1 million of murine breast cancer cells (4T1) were injected intramuscularly, in the mouse leg, 10 days before the treatment with oligo-His-PLGA NPs. The oligo-His-PLGA NPs

10.1002/anie.202011513

were injected directly into the tumour at a dose of 0.1 mmol/kg calculated on the base of the mmol of the oligo-His-PLGA polymer (MW=15300) administrated to the animal. Figure 5B shows that the relaxation rate increment measured at ca 1.33MHz was readily detectable, with ΔR_1 of 1.7 s^{-1}, corresponding to a 42.5% increase with respect to the relaxation rate measured at 1.65 MHz.

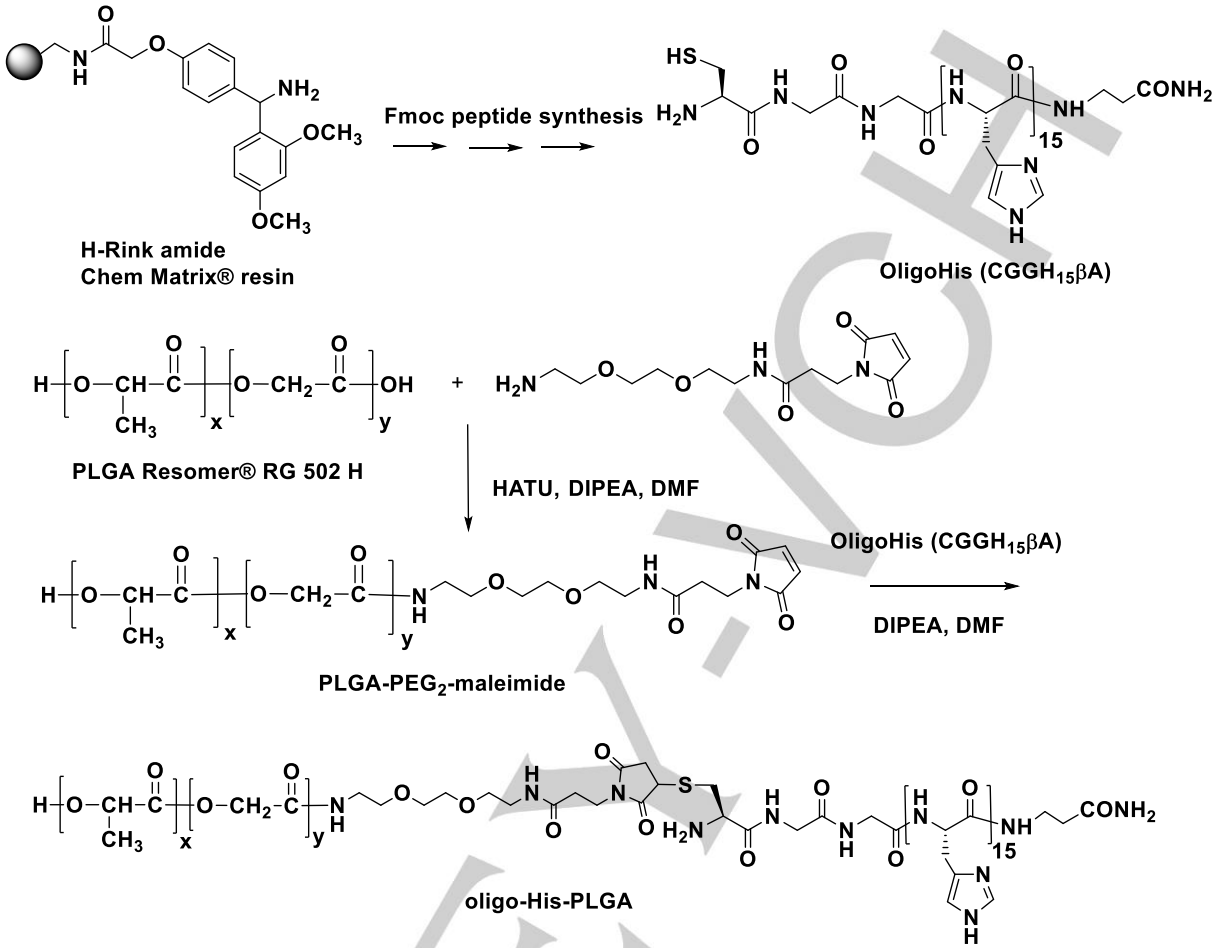

Figure 3. Synthesis scheme of oligo-His-PLGA. Schematic representation of the synthesis steps to obtain oligo-His-PLGA.

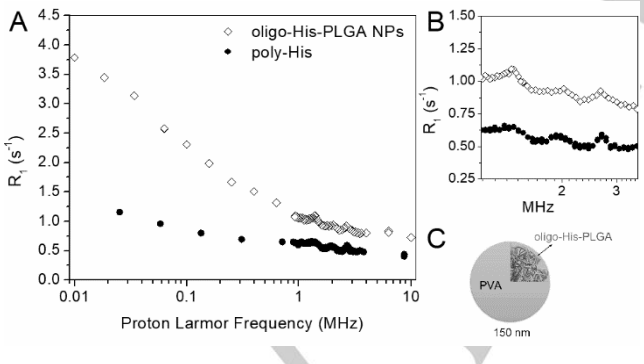

Figure 4. The oligo-His-PLGA-NP. (A) NMRD profiles of oligo-His-PLGA-NP (◊) in comparison to the commercial poly-His (●), at the same [His], i.e 5 mg/ml. (B) Expansion of the QP region. (C) Schematic representation of an oligo-His-PLGA NP. It was prepared according to the oil/water (o/w) emulsion solvent extraction method with PVA coating. See text for more details. Abbreviations: PLGA= Poly (Lactic-co-Glycolic Acid)-PEG2-Mal chain; PVA = PolyVinyl Alcohol.

On the contrary, the increase measured before the contrast agent injection at the same frequencies was not significantly different from zero. Due to the lower sensitivity of the surface coil, in order

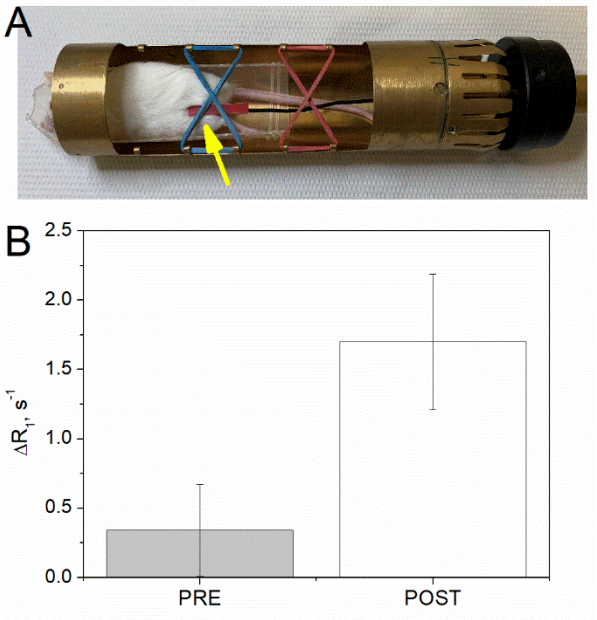

Figure 5. *In vivo* experiment with the oligo-His-PLGA NPs. (**A**) The mouse holder of the surface coil that fits within the wide-bore magnet of the FFC-

relaxometer. The arrow indicates the surface coil (from Voxalytic). (**B**) The relaxation rate differences acquired at 1.33 and 1.6 MHz PRE and POST the oligo-His-PLGA injection. The PRE data were acquired using two different coils, see text.

to obtain a sufficient signal-to-noise ratio it was necessary to average 4 scans, causing a marked increase of the acquisitiontime. These preliminary results demonstrate that the relaxation rate increase caused by this new polymeric (oligo-His-PLGA) contrast agent was readily detectable also after its "*in vivo*" injection.

Imaging of poly-Histidine nanoparticles by FFC Imager

The contrast generating ability of poly-His nanoparticles was assessed using a whole-body FFC MRI scanner. NMRD profiles obtained from whole sample non-imaging experiments are shown in Figure 6A. The NMRD profile obtained from oligo-His NPs show exogenous and endogenous QPs consistent with the relaxometry data. A contrast image was produced from the height of the QP (ΔR_1) at 33 mT (Figure 6B). The oligo-His NPs showed evident quadrupolar-induced relaxation differences compared to the blank nanoparticles. Region-of-interest analysis[31] of the contrast image (Figure 6C) yielded a greater positive image contrast (median (IQR) ΔR_1 of 0.095 (0.092 – 0.099) s^{-1}) from ologo-His nanoparticles compared to that obtained from the blank nanoparticles (ΔR_1 of 0.023 (0.021 – 0.033) s^{-1}).

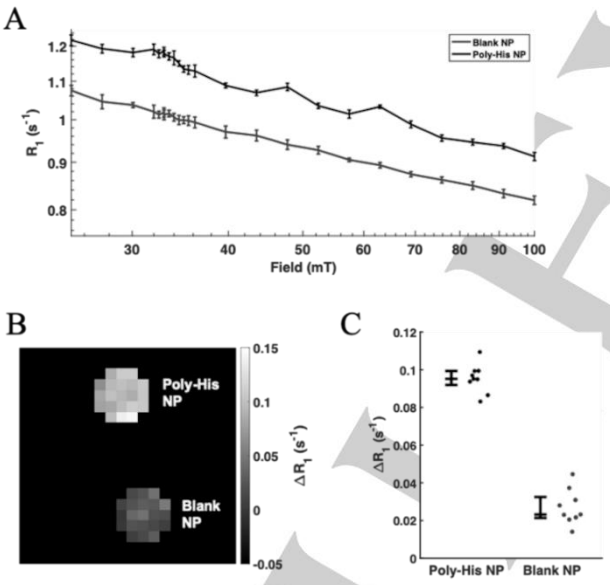

Figure 6. Imaging of Oligo-His NPs by FFC MRI. (**A**) NMR dispersion from single sample non-imaging experiment. Sample containing oligo-His NPs is shown in black. Sample containing nanoparticles without oligo-His (Blank NP) is shown in blue. Error bars represent the 95 % confidence interval obtained from each fit. (**B**) ΔR_1 image contrast obtained from the quadrupolar peak height at 33 mT with an in plane resolution of 2.19 x 2.19 mm. (**C**) Dot plot of the voxel ΔR_1 for each sample. Each dot represents a single value with each region-of-interest. The median and IQR value is indicated for each sample.

Discussion

The ability to measure water proton T_1 values over an extended range of magnetic field strengths introduces an entirely new dimension into biomedical NMR and MRI. By carrying out measurements as a function of magnetic field strength, completely new routes for obtaining contrast between normal and diseased tissues can be explored. The present study was designed to develop an innovative class of MRI contrast agents based on the generation of detectable ^{14}N-QPs that fall at frequencies that are readily distinguishable from those associated with the amidic peptide functionalities of endogenous tissue proteins whose ^{14}N-QPs fall at 0.7, 2.1 and 2.8 MHz, respectively. The observation of ^{14}N-QPs is strictly dependent on the immobilization in a gel state of the polymers containing the imidazolic moieties. In fact, ^{14}N-QPs are not seen in the case of isotropically-tumbling proteins or polymers, but their appearance requires that the molecular dynamics have to be slowed down on the time scale of the inverse quadrupole coupling constant (i.e. < 50 ns)[18]. Moreover, ^{14}N-^{1}H coupling concerns not only hydrogen atoms directly bound to nitrogen but also protons of the hydration water layer (about 55% of the exchangeable hydrogen nuclei that directly or indirectly sense the coupling interaction). Therefore, the water molecules forming the intermediate layer also have to be in a kind of slow-motion regime for them to transfer the ^{14}N-^{1}H relaxation to the "bulk" water. On this basis, the herein-considered imidazole-containing polymers were conjugated to biocompatible polymers such as polylactic and glycolic acid (PLGA), in order to form stable nanoparticles containing structured water in their inner cavities. Once administered *in vivo* these nanosized particles are expected to act as vascular and extra-vascular agents (in the presence of fenestrated capillaries), in analogy to what is observed for other NPs such as those based on iron oxides [32] or those based on PLGA containing GBCAs [33,34]. In addition, the ^{14}N-QPs of histidine-containing peptides may act as pH sensors, in turn providing valuable information on tumour cell metabolism. The measurement of tumour tissue pH has a marked prognostic relevance as the presence of slightly acidic zones (e.g. pH=6.6-6.8) surrounding hypoxic and necrotic areas is known to be an important factor in promoting cell migration and metastasis. Furthermore, an increase in poly-His mobility due to the pH decrease associated with cell death may also be detected in the case when the imidazole units are part of a scaffold matrix. In principle, one may envisage several conditions in which the overall dynamics of the imidazole-containing polymers could act as reporters of local physiological and pathological changes. The immobilization of the polymeric chains in a tissue-like state is mandatory for the generation of the ^{14}N-QPs and, since pH controls the physical state of the poly-His solid/liquid status, an estimate of the pH of the microenvironment in which the poly-His polymer is located can be acquired by the changes in the intensity of the imidazole QP.

The intensity of poly-His QPs is pH-dependent and its observation is possible only when poly-His is at pH > 6.6. This occurs because the transfer of the quadrupolar ^{14}N relaxation to the bulk water, which drives the bulk relaxation and produces the QPs, is only possible when water molecules are present in the hydration sphere of immobilised Poly-His polypeptide (with a tumbling time of the order of tens of nanoseconds) [16]. In this context, PLGA appear to be good candidates because of their ability to form rigid and water-permeable nanoparticles. In fact, QPs remain well

detectable when oligo-His moieties are embedded in the nanoparticles. In principle, PLGA can be replaced by other biocompatible polymers as the generation of the ^{14}N-QP at 1.38 MHz seems to be independent of the chemical compounds that constitute the semi-solid matrix in which the poly-His moiety is embedded.

The idea of developing MRI contrast agents based on the detection of QPs has also been recently tackled by Scharfetter *et al*.[35–37]. They investigated ^{209}Bi (I=9/2) containing organometallic compounds reporting interesting results that, however, appeared difficult to translate into living systems. Conversely, the poly-His containing compounds herein proposed are metal-free and highly biocompatible, biodegradable and non-toxic.

Conclusions

Access to the relaxation enhancement provided by the ^{14}N-QPs appears to offer a very promising approach to generate contrast in MR images. Imidazole showed itself to be a good candidate as it yields a ^{14}N-QP readily detectable from the naturally occurring ones, due to the amide functionalities of the semi-solid proteins. Contrary to the currently used GBCAs, this new class of agent is not represented by water-soluble molecules but rather has to be part of a solid system that restricts mobility. The physical form may range from water-suspended nanoparticles (as shown in this report) to bulkier devices such as cell-hosting scaffolds. The pH-responsiveness of the ^{14}N-QP generated by imidazole moieties appears to be an important property that allows the design of systems able to sense the local pH, which can then act as reporters of pathological conditions that are known to affect the local pH. As the effect of imidazole ^{14}N-QP is detected at 1.38 MHz, this implies that it cannot be observed on current clinical MRI scanners. Fast Field Cycling imagers are needed for its exploitation and one may expect that the results reported here may be useful for further accelerating the development of the next generation of instruments based on the acquisition of MR images over an extended range of magnetic fields.[19]

Acknowledgements

This project has received funding from the European Union Horizon 2020 research and innovation programme under grant agreement No 668119 (project “IDentIFY”) and from the ATTRACT project funded by the EC under Grant Agreement No. 777222. This work was performed in the frame of the COST Action AC15209 (EURELAX). The Italian Ministry for Education and Research (MIUR) is gratefully acknowledged for yearly FOE funding to the Euro-BioImaging Multi-Modal Molecular Imaging Italian Node (MMMI).

Keywords: . Magnetic Resonance Imaging, Contrast Agents, ^{14}N quadrupolar peaks, Fast Field Cycling, nanoparticles

[1] J. Wahsner, E. M. Gale, A. Rodríguez-Rodríguez, P. Caravan, *Chem. Rev.* **2019**, *119*, 957–1057.

[2] E. Terreno, W. Dastrù, D. D. Castelli, E. Gianolio, S. G. Crich, D. Longo, S. Aime, *Curr. Med. Chem.* **2010**, *17*, DOI 10.2174/092986710793213823.

[3] J. Lohrke, T. Frenzel, J. Endrikat, F. C. Alves, T. M. Grist, M. Law, J. M. Lee, T. Leiner, K.-C. Li, K. Nikolaou, M. R. Prince, H. H. Schild, J. C. Weinreb, K. Yoshikawa, H. Pietsch, *Adv. Ther.* **2016**, *33*, 1–28.

[4] T. J. Clough, L. Jiang, K. L. Wong, N. J. Long, *Nat. Commun.* **2019**, *10*, 1–14.

[5] T. Kanda, K. Ishii, H. Kawaguchi, K. Kitajima, D. Takenaka, *Radiology* **2014**, *270*, 834–41.

[6] A. J. van der Molen, P. Reimer, I. A. Dekkers, G. Bongartz, M. F. Bellin, M. Bertolotto, O. Clement, G. Heinz-Peer, F. Stacul, J. A. W. Webb, H. S. Thomsen, *Eur. Radiol.* **2018**, *28*, 2845–2855.

[7] E. Di Gregorio, G. Ferrauto, C. Furlan, S. Lanzardo, R. Nuzzi, E. Gianolio, S. Aime, *Invest. Radiol.* **2018**, *53*, 167–172.

[8] E. Di Gregorio, R. Iani, G. Ferrauto, R. Nuzzi, S. Aime, E. Gianolio, *J. Trace Elem. Med. Biol.* **2018**, *48*, 239–245.

[9] M. Botta, F. Carniato, D. Esteban-Gómez, C. Platas-Iglesias, L. Tei, *Future Med. Chem.* **2019**, *11*, 1461–1483.

[10] P. Mathieu, Y. Coppel, M. Respaud, Q. T. Nguyen, S. Boutry, S. Laurent, D. Stanicki, C. Henoumont, F. Novio, J. Lorenzo, D. Montpeyó, C. Amiens, *Molecules* **2019**, *24*, DOI 10.3390/molecules24244629.

[11] R. Botár, E. Molnár, G. Trencsényi, J. Kiss, F. K. Kálmán, G. Tircsó, *J. Am. Chem. Soc.* **2020**, *142*, 1662–1666.

[12] L. M. Broche, G. P. Ashcroft, D. J. Lurie, *Magn. Reson. Med.* **2012**, *68*, 358–362.

[13] L. M. Broche, S. R. Ismail, N. A. Booth, D. J. Lurie, *Magn. Reson. Med.* **2012**, *67*, 1453–7.

[14] F. Winter, R. Kimmich, *BBA - Gen. Subj.* **1982**, *719*, 292–298.

[15] S. H. Koenig, *Acad. Radiol.* **1996**, *3*, 597–606.

[16] B. Halle, *Magn. Reson. Med.* **2006**, *56*, 60–72.

[17] P. H. Fries, E. Belorizky, *J. Chem. Phys.* **2015**, *143*, DOI 10.1063/1.4926827.

[18] E. P. Sunde, B. Halle, *J. Magn. Reson.* **2010**, *203*, 257–73.

[19] L. M. Broche, P. J. Ross, G. R. Davies, M. J. MacLeod, D. J. Lurie, *Sci. Rep.* **2019**, *9*, 10402.

[20] D. J. Lurie, S. Aime, S. Baroni, N. A. Booth, L. M. Broche, C. H. Choi, G. R. Davies, S. Ismail, D. Ó hÓgáin, K. J. Pine, *Comptes Rendus Phys.* **2010**, *11*, 136–148.

[21] X. Jiao, R. G. Bryant, *Magn. Reson. Med.* **1996**, *35*, 159–161.

[22] M. L. S. Garcia, J. A. S. Smith, P. M. G. Bavin, C. R. Ganellin, *J. Chem. Soc. Perkin Trans. 2* **1983**, 1391–1399.

[23] Q. Tang, D. Zhao, H. Yang, L. Wang, X. Zhang, *J. Mater. Chem. B* **2019**, *7*, 30–42.

[24] M. P. McCurdie, L. A. Belfiore, *J. Polym. Sci. Part B Polym. Phys.* **1999**, *37*, 301–309.

[25] M. Mir, N. Ahmed, A. ur Rehman, *Colloids Surfaces B Biointerfaces* **2017**, *159*, 217–231.

[26] F. Molavi, M. Barzegar-Jalali, H. Hamishehkar, *J. Control. Release* **2020**, *320*, 265–282.

[27] R. N. Mariano, D. Alberti, J. C. Cutrin, S. G. Crich, S. Aime, *Mol. Pharm.* **2014**, *11*, DOI 10.1021/mp5002747.

[28] L. N. Turino, M. R. Ruggiero, R. Stefanìa, J. C. Cutrin, S. Aime, S. Geninatti Crich, *Bioconjug. Chem.* **2017**, *28*, DOI 10.1021/acs.bioconjchem.7b00096.

[29] S. K. Sahoo, J. Panyam, S. Prabha, V. Labhasetwar, *J. Control. Release* **2002**, *82*, 105–114.

[30] M. R. Ruggiero, S. Baroni, S. Pezzana, G. Ferrante, S. Geninatti

Crich, S. Aime, *Angew. Chemie - Int. Ed.* **2018**, *57*, DOI 10.1002/anie.201713318.

[31] L. M. Broche, P. J. Ross, G. R. Davies, D. J. Lurie, *Magn. Reson. Imaging* **2017**, *44*, 55–59.

[32] G. B. Toth, C. G. Varallyay, A. Horvath, M. R. Bashir, P. L. Choyke, H. E. Daldrup-Link, E. Dosa, J. P. Finn, S. Gahramanov, M. Harisinghani, I. Macdougall, A. Neuwelt, S. S. Vasanawala, P. Ambady, R. Barajas, J. S. Cetas, J. Ciporen, T. J. DeLoughery, N. D. Doolittle, R. Fu, J. Grinstead, A. R. Guimaraes, B. E. Hamilton, X. Li, H. L. McConnell, L. L. Muldoon, G. Nesbit, J. P. Netto, D. Petterson, W. D. Rooney, D. Schwartz, L. Szidonya, E. A. Neuwelt, *Kidney Int.* **2017**, *92*, 47–66.

[33] G. Rigaux, V. G. Roullin, C. Cadiou, C. Portefaix, L. Van Gulick, G. Bœuf, M. C. Andry, C. Hoeffel, L. Vander Elst, S. Laurent, R. Muller, M. Molinari, F. Chuburu, *Nanotechnology* **2014**, *25*, 445103.

[34] D. Alberti, N. Protti, M. Franck, R. Stefania, S. Bortolussi, S. Altieri, A. Deagostino, S. Aime, S. Geninatti Crich, *ChemMedChem* **2017**, *12*, 502–509.

[35] D. Kruk, E. Umut, E. Masiewicz, C. Sampl, R. Fischer, S. Spirk, C. Goesweiner, H. Scharfetter, *Phys. Chem. Chem. Phys.* **2018**, *20*, 12710–12718.

[36] D. Kruk, E. Masiewicz, E. Umut, A. Petrovic, R. Kargl, H. Scharfetter, *J. Chem. Phys.* **2019**, *150*, 184306.

[37] C. Gösweiner, P. Lantto, R. Fischer, C. Sampl, E. Umut, P. O. Westlund, D. Kruk, M. Bödenler, S. Spirk, A. Petrovič, H. Scharfetter, *Phys. Rev. X* **2018**, *8*, 021076.

10.1002/anie.202011513

WILEY-VCH

RESEARCH ARTICLE

Entry for the Table of Contents

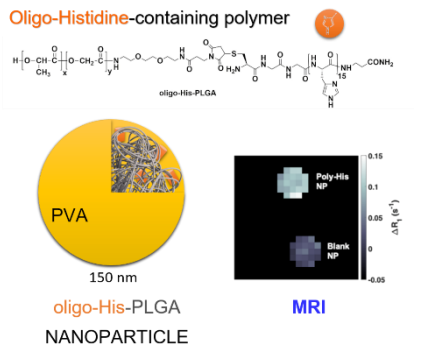

Insert text for Table of Contents here. In this study, we developed completely new, metal free, MRI contrast agents that differ completely from current clinical contrast agents, which contain potentially toxic paramagnetic metals. These sensors enhance image contrast thanks to the 14N of imidazole groups of histidine, which are conjugated to the PLGA polymeric chains forming pH-sensitive, biocompatible and biodegradable nanoparticles.